[20] H. M. Srivastava, K. C. Gupta, and S. P. Goyal, *The H-Functions of One and Two Variables With Applications*. New Delhi, India: South Asian Publishers, 1982.
[21] A. M. Mathai and R. K. Saxena, "Expansion of Meijer's G-function of two variables when the upper parameters differ by integers," *Kyungpook Math. J.*, vol. 12, no. 1, pp. 61–68, Jun. 1972.
[22] I. S. Ansari, S. Al-Ahmadi, F. Yilmaz, M.-S. Alouini, and H. Yanikomeroglu, "A new formula for the BER of binary modulations with dual-brance selection over gereralized-K composite fading channels," *IEEE Trans. Commun.*, vol. 59, no. 10, pp. 2654–2658, Oct. 2011.
[23] J. L. Burchnall and T. W. Chaundy, "Expansion of Appell's double hypergeometric functions," *Quart. J. Math. (Oxford)*, vol. 11, pp. 249–270, Nov. 1940.
[24] Y. Li and S. Kishore, "Asymptotic analysis of amplify-and-forward relaying in Nakagami-fading environments," *IEEE Trans. Wireless Commun.*, vol. 6, no. 12, pp. 4256–4262, Nov. 2007.

Optimal Phase Response Functions for Fast Pulse-Coupled Synchronization in Wireless Sensor Networks

Yongqiang Wang and Francis J. Doyle, III

***Abstract*—Synchronization is crucial to wireless sensor networks. Recently, a pulse-coupled synchronization strategy that emulates biological pulse-coupled agents has been used to achieve this goal. We propose to optimize the phase response function such that synchronization rate is maximized. Since the synchronization rate is increased independently of transmission power, energy consumption is reduced, hence extending the life of battery-powered sensor networks. A comparison with existing phase response functions confirms the effectiveness of the method.**

***Index Terms*—Phase response function, pulse-coupled oscillators, synchronization rate, wireless sensor networks.**

I. Introduction

Pulse-coupled oscillators (PCOs) have received increased attention in past decades. It is an effective tool to describe many biological synchronization phenomena such as the flashing of fireflies, the contraction of cardiac cells and the firing of neurons [1], [2]. Due to its importance in biological oscillations, PCOs have been extensively studied in the life science literature [3].

Recently, the PCO based synchronization strategy has been applied to wireless sensor networks. In pulse-coupled synchronization strategy, each sensor marks its individual time slot starting point by sending a pulse, and by adjusting its state upon receiving a pulse from adjacent nodes, the whole network can be synchronized [4]–[6]. Since PCOs can be synchronized via pulse transmitting instead of packet exchanging, it avoids wasting the limited computational capability of sensor nodes which is required by packet based synchronization algorithms. Moreover, the pulse-coupled synchronization strategy does not require any memory to store the information of neighboring nodes, which is of great appeal to low cost sensor nodes. Therefore, the PCO based synchronization scheme has received increased attention in the communication community recently. For example, the authors in [5] discussed the implementation of PCOs in a wide band network, the authors in [7] verified the effectiveness of PCO based synchronization strategy using a TinyOS simulator. The authors in [8] and [9] discussed the scalability of pulse-coupled strategy when used to synchronize sensor networks. The authors in [10] and [11] gave the maximal allowable refractory period of PCOs when applied to synchronize wireless sensor networks.

In PCOs, oscillators interact in a pulsatile rather than a smooth manner. This effect can be captured as a phase response function [12]. The phase response function tabulates the shift in the phase of an oscillation induced by a perturbation as a function of the phase at which the perturbation is received. It has been proven to play an important role in the synchronization process [3], [12]–[16]. However, in published applications of pulse-coupled strategies to wireless sensor network synchronization, the phase response function is not strategically designed. We propose to optimize the phase response function such that the synchronization rate is maximized. Given that energy consumption in the synchronization process is determined by the product of transmission power and time to synchronization, which correspond to coupling strength and synchronization rate, respectively, our optimal phase response function saves the energy consumed in the synchronization process since it is independent of coupling strength. This has great significance in wireless sensor networks, where sensors are typically battery driven.

II. Problem Formulation and Model Transformation

Consider N pulse-coupled oscillators $\dot{x}_i = f_i(x_i)$ where f_i is the dynamics and $x_i \in [0,1]$ is the state ($i = 1,2\ldots,N$). When x_i reaches 1, oscillator i fires (emits a pulse) and resets x_i to 0. When oscillator i receives a pulse from an adjacent oscillator (e.g., oscillator j), it shifts x_i to $x_i + l$ or 1, whichever is less, i.e., [2]

$$x_j(t) = 1 \Longrightarrow x_i(t^+) = \min\{1, x_i(t) + l\}, \quad l \in (0,1] \tag{1}$$

The shift in state can be modeled by a Dirac function $\delta(t)$, which is zero for all values of t except $t = 0$ and satisfies $\int_{-\infty}^{\infty} \delta(t)dt = 1$. The coupled dynamics is given by [12]:

$$\dot{x}_i = f_i(x_i) + \sum_{1 \le j \le N, j \ne i} l a_{i,j} \delta(t - t_j), \quad i = 1,2,\ldots,N \tag{2}$$

where $a_{ij} \in \{0,1\}$ denotes the effect of oscillator j on oscillator i: when x_j reaches 1 (at t_j), oscillator j fires and resets x_j to 0, and at the same time pulls oscillator i up by an amount $la_{i,j}$.

Remark 1: If $a_{i,j}$ is 0, then oscillator i is not affected by oscillator j.

Assumption 1: We assume that the interaction is bidirectional, i.e., $a_{i,j} = a_{j,i}$, which is common in wireless networks [17]. We also assume that the interaction topology is connected, i.e., there is a multi-hop path (i.e., a sequence with nonzero values a_{i,m_1}, $a_{m_1,m_2},\ldots,a_{m_{p-1},m_p}, a_{m_p,j}$) from each node i to every other node j.

Assumption 2: We assume that the coupling is weak, i.e., $l \ll 1$ [15].

Manuscript received May 05, 2012; accepted June 27, 2012. Date of publication July 11, 2012; date of current version September 11, 2012. The associate editor coordinating the review of this manuscript and approving it for publication was Prof. YaoWin (Peter) Hong. The work was supported in part by the U.S. Army Research Office through Grant W911NF-07-1-0279, National Institutes of Health through Grant GM078993, and the Institute for Collaborative Biotechnologies through grant W911NF-09-0001 from the U.S. Army Research Office. The content of the information does not necessarily reflect the position or the policy of the Government, and no official endorsement should be inferred.

The authors are with the Institute for Collaborative Biotechnologies, University of California, Santa Barbara, CA 93106-5080 USA (e-mail: wyqthu@gmail.com; frank.doyle@icb.ucsb.edu).

Color versions of one or more of the figures in this paper are available online at http://ieeexplore.ieee.org.

Digital Object Identifier 10.1109/TSP.2012.2208109

Based on Assumption 2, (2) can be transformed into a phase model using phase reduction techniques and phase averaging techniques [12], [15], [18]:

$$\dot{\theta}_i = w_i + \sum_{1\le j\le N, j\neq i} l a_{i,j} Q(\theta_j - \theta_i), \quad i = 1, 2, \ldots, N \tag{3}$$

where $\theta_i \in [0, 2\pi)$ and w_i denote the phase and natural frequency of oscillator i, respectively. $Q(-\varphi) = F(\varphi)$ is the phase response function as defined in Definition 1:

Definition 1 [12]: Phase response function $F(\varphi)$ is the phase shift induced by a pulse under coupling strength $l = 1$, i.e., $F(\varphi) \triangleq \varphi_{\text{new}} - \varphi$, with φ_{new} and φ denote the respective phase after and before pulsing perturbation under coupling strength $l = 1$. $F(\varphi)$ is 2π-periodic.

Remark 2: The transformation from (2) to (3) is a standard practice in the study of weakly connected PCOs and it is applicable to any limit-cycle oscillation function f_i and f_g [12]. The detailed procedure has been well documented in [19], Chapter 9 of [15], and Chapter 10 of [12].

In all existing pulse-coupled synchronization strategies for wireless sensor networks, the phase response function $F(\varphi)$ (i.e., $Q(-\varphi)$) is not strategically designed. In the paper, we propose to increase the synchronization rate of wireless sensor networks by exploiting the design freedom in $F(\varphi)$, more specifically, we are interested in the optimal form of $F(\varphi)$ that maximizes the synchronization rate (The synchronization rate determines energy consumption in sensor network synchronization, and it is an important metric for many other oscillator networks as well [20]). As shown in [14], advance-and-delay phase response functions outperform advance-only phase response functions, so we make the following assumption:

Assumption 3: $F(\varphi)$ is odd, i.e., $F(-\varphi) = -F(\varphi)$ holds, and thus $Q(-\varphi) = -Q(\varphi)$ holds.

III. Optimal Phase Response Function in the Identical Natural Frequency Case

When the natural frequencies are identical, i.e., $w_1 = w_2 = \cdots = w_N = w$, (3) reduces to

$$\dot{\theta}_i = w + \sum_{1\le j\le N, j\neq i} l a_{i,j} Q(\theta_j - \theta_i), \quad i = 1, 2, \ldots, N \tag{4}$$

To find the phase response function that maximizes the synchronization rate, we first study how the phase response function affects the synchronization rate. The result is detailed in Theorem 1:

Theorem 1: For the oscillator network in (4), when $\theta_{\max} \triangleq \max_i\{\theta_i\}$ and $\theta_{\min} \triangleq \min_i\{\theta_i\}$ satisfy $\theta_{\max} - \theta_{\min} < \pi$, if $\frac{Q(\varphi)}{\varphi} > 0$ holds for $-\pi < \varphi < \pi$, then the oscillators will synchronize, and the synchronization rate is maximized when $\frac{Q(\varphi)}{\varphi}$ is maximized.

Proof: Since the interaction is bidirectional and $Q(\varphi)$ is an odd function, we have $\sum_{i=1}^N \dot{\theta}_i = Nw$ from (4), which leads to $\frac{1}{N}\sum_{i=1}^N \theta_i = wt + \alpha$ where α is a constant. Hence, the difference between θ_i and the mean value $\frac{1}{N}\sum_{i=1}^N \theta_i$ can be represented by $\phi_i = \theta_i - \frac{1}{N}\sum_{i=1}^N \theta_i = \theta_i - (wt + \alpha)$. So phases θ_i synchronize if and only if all ϕ_i are identical. From the definitions of ϕ_i, we have $\sum_{i=1}^N \phi_i = 0$, and thus the phases synchronize if and only if all ϕ_i are 0.

Next we prove that ϕ_i will converge to 0 when $\frac{Q(\varphi)}{\varphi} > 0$ holds for $-\pi < \varphi < \pi$.

Substituting $\theta_i = wt + \alpha + \phi_i$ into (4) gives the dynamics of ϕ_i:

$$\dot{\phi}_i = \sum_{1\le j\le N, j\neq i} l a_{i,j} Q(\phi_j - \phi_i), \quad i = 1, 2, \ldots, N \tag{5}$$

Define a Lyapunov function as $V = \frac{1}{2}\Phi^T\Phi$, where $\Phi = [\phi_1, \phi_2, \ldots, \phi_N]^T$. $V \ge 0$ will be 0 if and only if all ϕ_i are zero, meaning that the network is synchronized.

Differentiating V along the trajectories of (5) yields

$$\begin{aligned}
\dot{V} = \Phi^T\dot{\Phi} &= l\sum_{i=1}^N \sum_{1\le j\le N, j\neq i} a_{i,j}\phi_i Q(\phi_j - \phi_i) \\
&= l \sum_{1\le i,j\le N, i<j} a_{i,j}\left(\phi_i Q(\phi_j - \phi_i) + \phi_j Q(\phi_i - \phi_j)\right) \\
&= -l \sum_{1\le i,j\le N, i<j} a_{i,j}(\phi_i - \phi_j) Q(\phi_i - \phi_j) \\
&= -l \sum_{1\le i,j\le N, i<j} a_{i,j}\frac{Q(\phi_i - \phi_j)}{\phi_i - \phi_j}(\phi_i - \phi_j)^2
\end{aligned} \tag{6}$$

In (6), the initial value of $\phi_i - \phi_j$ resides in $(-\pi, \pi)$ since $\phi_i - \phi_j = \theta_i - \theta_j$ and $\theta_{\max} - \theta_{\min} < \pi$ hold. From the assumption $\frac{Q(\varphi)}{\varphi} > 0$ on $(-\pi, \pi)$, we have $Q(\varphi) \ge 0$ on $[0, \pi)$ and $Q(\varphi) \le 0$ on $(-\pi, 0]$. Given that $\phi_{\max} \triangleq \max_i\{\phi_i\}$ and $\phi_{\min} \triangleq \min_i\{\phi_i\}$ satisfy $0 \ge \phi_j - \phi_{\max} > -\pi$ and $\pi > \phi_j - \phi_{\min} \ge 0$, respectively, we have $\dot{\phi}_{\max} \le 0$ and $\dot{\phi}_{\min} \ge 0$ from (5). Therefore, $\phi_{\max} - \phi_{\min}$ will always reside in $[0, \pi)$ in its evolution, and hence, $\phi_i - \phi_j$ in (6) always resides in $(-\pi, \pi)$, on which $\frac{Q(\varphi)}{\varphi} > 0$ holds. Given that the interaction topology $a_{i,j}$ is connected, it follows that $\dot{V} \le 0$ holds and $\dot{V} = 0$ implies the equality of all ϕ_i. Recall $\sum_{i=1}^N \phi_i = 0$, so $\dot{V} = 0$ implies $\Phi = 0$. In other words, $\Phi \neq 0$ implies $\dot{V} < 0$. Therefore, if $\frac{Q(\varphi)}{\varphi} > 0$ holds, V, and hence Φ, will decay to 0, meaning that all θ_i will synchronize.

Next we proceed to consider the synchronization rate. The synchronization rate is determined by the rate at which Φ decays to 0. To get the decay rate of Φ, we rewrite (6) as follows:

$$\dot{V} = -l\Phi^T L\Phi \tag{7}$$

with L constructed as follows: for $i \neq j$, its (i,j)th element is $-l a_{i,j}\frac{Q(\phi_i - \phi_j)}{\phi_i - \phi_j}$, for $i = j$, its (i,j)th element is $\sum_{1\le m\le N, m\neq i} l a_{i,m}\frac{Q(\phi_i - \phi_m)}{\phi_i - \phi_m}$. L can be regarded as a weighted Laplacian of the interaction topology [21]. Hence when $\frac{Q(\varphi)}{\varphi} > 0$, L is positive semidefinite and the decay rate of ϕ_i is given by the second smallest eigenvalue $\lambda_2(L)$ (note that since $\Phi^T\mathbf{1} = 0$ holds for $\mathbf{1} \triangleq [1, 1, \ldots, 1]^T$, Φ is orthogonal to $\mathbf{1}$, which corresponds to L's smallest eigenvalue 0 [21]). From the Courant-Weyl inequalities (see, e.g., Chapter 2 of [21]), we know $\lambda_2(L)$ is an increasing function of any $l a_{i,j}\frac{Q(\phi_i - \phi_j)}{\phi_i - \phi_j}$ and hence an increasing function of $\frac{Q(\varphi)}{\varphi}$. So the synchronization rate increases with $\frac{Q(\varphi)}{\varphi}$, and the maximal synchronization rate is attained when $\frac{Q(\varphi)}{\varphi}$ is maximized. ■

Remark 3: In Theorem 1, the phase difference needs to be less than π, this is because $Q(\varphi)$'s periodicity and oddness give (5) non-in-phase equilibria, which prevent global convergence to synchronization over the whole phase space [22] (Note that [2] and [7] have shown that for some initial conditions—even with measure zero—, PCOs cannot be synchronized even under all-to-all connection). Moreover, a less than π phase difference is practical in sensor networks due to limited clock drift [7]. Furthermore, even if this is not satisfied, a simple initial flood (cf. [23] for flooding algorithms) can bring all nodes to within a small phase difference quickly [7].

Theorem 1 shows that by designing $Q(\varphi)$, synchronization rate can be increased, even with coupling strength l fixed. Next, we derive the optimal $Q(\varphi)$ to maximize the synchronization rate. The optimal phase response function solves the following optimization problem:

$$\max_{Q(\varphi)} \frac{Q(\varphi)}{\varphi} \text{ subject to } \begin{cases} -Q(\varphi) + \varphi < 2\pi \\ -Q(\varphi) + \varphi \ge 0 \end{cases} \tag{8}$$

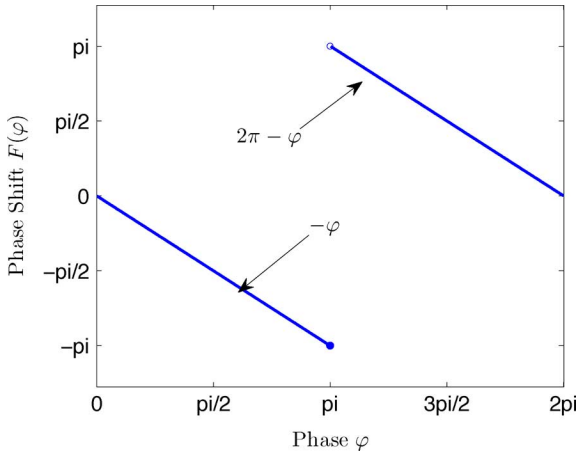

Fig. 1. The optimal phase response function for oscillators with identical natural frequencies.

The constraints come from the assumption $Q(\varphi) = F(-\varphi) = -F(\varphi)$ and the fact that under unit coupling strength ($l = 1$), the phase after pulsing perturbation (i.e., $\varphi + F(\varphi)$) still resides in the interval $[0, 2\pi)$. It guarantees that $F(\varphi)$ is a single-valued function.

The optimal phase response function that solves (8) is given in Theorem 2.

Theorem 2: For PCOs with identical natural frequencies and $\theta_{\max} - \theta_{\min} < \pi$, the optimal phase response function $F(\varphi)$ that maximizes the synchronization rate is given by

$$F(\varphi) = \begin{cases} -\varphi & 0 \le \varphi \le \pi \\ 2\pi - \varphi & \pi < \varphi < 2\pi \end{cases} \tag{9}$$

Proof: From Theorem 1, we need to prove that (9) maximizes $\frac{Q(\varphi)}{\varphi}$ for $-\pi < \varphi < \pi$. Since $Q(\varphi) = F(-\varphi)$ is odd, we only need to prove that $Q(x)$ maximizes $\frac{Q(\varphi)}{\varphi}$ on $0 < \varphi < \pi$.

For any $0 < \varphi < \pi$, because φ is non-negative, $\frac{Q(\varphi)}{\varphi}$ is maximized when $Q(\varphi)$ is maximized. Given that $Q(\varphi)$ is constrained in $(\varphi - 2\pi, \varphi]$ for any $0 < \varphi < \pi$ according to (8), we know the optimal $Q(\varphi)$ that maximizes the synchronization rate is given by $Q(\varphi) = \varphi$ when $0 < \varphi < \pi$.

For $\varphi = 0$ (corresponding to $\phi_i = \phi_j$ in the proof of Theorem 1), the value of $Q(\varphi)$ does not affect the synchronization rate since all ϕ_i are already synchronized. So $Q(0) = 0$ is adopted to guarantee the continuity of $Q(\varphi)$ and the stability of the synchronization manifold [5], [12].

For $\varphi = \pi$, $Q(\pi) = \pi$ is adopted to guarantee the continuity of $Q(\varphi)$ on $[0, \pi]$. ∎

The optimal phase response function is visualized in Fig. 1.

IV. Optimal Phase Response Function in the Non-Identical Natural Frequency Case

When oscillators have non-identical natural frequencies, their phases may not be synchronized [24]. In this section, we will show that their oscillating frequencies can be synchronized under certain conditions and the synchronization rate can be maximized by optimizing the phase response function. It is worth noting that frequency synchronization is extremely beneficial for wireless communication since it enables the use of cooperative diversity techniques such as distributed space-time codes [25]. It is also crucial for collaborative communication systems in that it increases data throughput and robustness to signal fading [26].

When natural frequencies are non-identical, the oscillators' phase dynamics are given by (3).

Assumption 4: We assume that the natural frequencies w_i are constant with respect to time.

Theorem 3: For the oscillator network in (3), when Assumption 4 holds, their oscillating frequencies synchronize if $Q'(\varphi) \triangleq \frac{dQ(\varphi)}{d\varphi}$ is positive for $-2\pi < \varphi < 2\pi$, and the synchronization rate is maximized when $Q'(\varphi)$ is maximized.

Proof: The oscillating frequency of oscillator i is $\vartheta_i \triangleq \dot{\theta}_i$. As shown in (3), it is affected by both natural frequency w_i and inter-oscillator coupling. Differentiating (3) yields its dynamics:

$$\dot{\vartheta}_i = \sum_{1 \le j \le N, j \ne i} l a_{i,j} Q'(\theta_j - \theta_i)(\vartheta_j - \vartheta_i), \quad i = 1, 2, \ldots, N \tag{10}$$

Since the interaction is bidirectional and Q' is an even function (the derivative of an odd function is an even function [18]), we have $\sum_{i=1}^{N} \dot{\vartheta}_i = 0$ from (10), which leads to $\frac{1}{N}\sum_{i=1}^{N} \vartheta_i = \beta$ where β is a constant. Hence, the difference between ϑ_i and the mean value $\frac{1}{N}\sum_{i=1}^{N} \vartheta_i$ can be represented by $\xi_i = \vartheta_i - \frac{1}{N}\sum_{i=1}^{N} \vartheta_i = \vartheta_i - \beta$. Oscillating frequencies ϑ_i synchronize if and only if all ξ_i are identical. From the definitions of ξ_i, we have $\sum_{i=1}^{N} \xi_i = 0$, and thus the oscillating frequencies synchronize if and only if all ξ_i are 0.

Now we prove that ξ_i will converge to 0 when $Q'(\varphi) > 0$ holds for $-2\pi < \varphi < 2\pi$.

Substituting $\vartheta_i = \beta + \xi_i$ into (10) gives the dynamics of ξ_i:

$$\dot{\xi}_i = \sum_{1 \le j \le N, j \ne i} l a_{i,j} Q'(\theta_j - \theta_i)(\xi_j - \xi_i), \quad i = 1, 2, \ldots, N \tag{11}$$

Define a Lyapunov function as $V = \frac{1}{2}\Xi^T\Xi$, where $\Xi = [\xi_1, \xi_2, \ldots, \xi_N]^T$. $V \ge 0$ will be 0 if and only if all ξ_i are 0, meaning that the oscillating frequencies $\vartheta_i = \beta + \xi_i$ are synchronized.

Similar to (6), differentiating V along the trajectories of (11) yields

$$\begin{aligned} \dot{V} = \Xi^T\dot{\Xi} &= l\sum_{i=1}^{N} \sum_{1 \le j \le N, j \ne i} a_{i,j}\xi_i Q'(\theta_j - \theta_i)(\xi_j - \xi_i) \\ &= -l \sum_{1 \le i,j \le N, i<j} a_{i,j} Q'(\theta_i - \theta_j)(\xi_i - \xi_j)^2 \end{aligned} \tag{12}$$

So we know when $Q'(\varphi)$ is positive in $(-2\pi, 2\pi)$ (the range of $\theta_i - \theta_j$) and the interaction topology $a_{i,j}$ is connected, $\dot{V} \le 0$ holds, and $\dot{V} = 0$ implies that all ξ_i are identical. Recall that $\sum_{i=1}^{N} \xi_i = 0$, so $\dot{V} = 0$ implies $\Xi = 0$. In other words, $\Xi \ne 0$ implies $\dot{V} < 0$. Therefore, V, and hence Ξ, will decay to 0, meaning that the oscillating frequencies $\vartheta_i = \dot{\theta}_i$ will synchronize.

To get the synchronization rate of oscillating frequencies, we rewrite (12) as follows:

$$\dot{V} = -l\Xi^T M \Xi \tag{13}$$

with M constructed as follows: for $i \ne j$, its (i,j)th element is $-l a_{i,j} Q'(\theta_i - \theta_j)$, for $i = j$, its (i,j)th element is $\sum_{1 \le m \le N, m \ne i} l a_{i,m} Q'(\theta_i - \theta_m)$. M can be regarded as a weighted Laplacian of the interaction topology [21]. Hence when $Q'(\varphi) > 0$, M is positive semidefinite and the decay rate of ξ_i is given by the second smallest eigenvalue $\lambda_2(M)$ (note that since $\Xi^T\mathbf{1} = 0$, Ξ is orthogonal to $\mathbf{1}$, which corresponds to M's smallest eigenvalue 0 [21]). From the Courant-Weyl inequalities (see, e.g., Chapter 2 of [21]), we know $\lambda_2(M)$ is an increasing function of any $l a_{i,j} Q'(\theta_i - \theta_j)$ and hence an increasing function of $Q'(\varphi)$. Therefore, the rate of frequency synchronization increases with an increase in $Q'(\varphi)$, and it is maximized when $Q'(\varphi)$ is maximized. ∎

Remark 4: Note that $\theta_i - \theta_j$ and hence $Q'(\theta_i - \theta_j)$ in (12) keep changing with time if oscillating frequencies are not synchronized, so

if $Q'(\varphi) = 0$ holds for some single φ (at which $\dot{V} = 0$), V will not be retained at this point and can still converge to 0, hence ϑ_i will still synchronize.

Similar to Section III, by optimizing the phase response function, we can maximize the rate of frequency synchronization even with coupling strengths fixed, hence we can reduce energy consumption in synchronization. Since the algebraic derivation used in the preceding section cannot be used anymore, we propose to solve the following optimization problem:

$$\max_{Q(\varphi)} \int_{-\pi}^{\pi} Q'^2(\varphi)d\varphi \text{ subject to } \int_{-\pi}^{\pi} Q^2(\varphi)d\varphi = C \tag{14}$$

where C is a constant. The constraint in (14) is used to normalize the phase response function.

Equation (14) can be considered as a variational problem minimizing the functional form

$$\begin{aligned} A[Q] &= \int_{-\pi}^{\pi} \mathcal{L}(Q(\varphi), \varphi)d\varphi \\ &= \int_{-\pi}^{\pi} -Q'^2(\varphi) + \lambda\left(Q^2(\varphi) - C/(2\pi)\right)d\varphi \end{aligned} \tag{15}$$

According to Euler-Lagrange equation, the optimal $Q(\varphi)$ satisfies

$$\frac{\partial \mathcal{L}}{\partial Q} - \frac{d}{d\varphi}\frac{\partial \mathcal{L}}{\partial Q'} = 0 \tag{16}$$

Substituting $\mathcal{L}(Q(\varphi), \varphi)$ in (15) into (16) yields

$$2\lambda Q(\varphi) + 2\frac{d^2Q(\varphi)}{d^2\varphi} = 0$$

Therefore, the optimal $Q(\varphi)$ has a form of

$$Q(\varphi) = a_1 e^{\sqrt{-\lambda}\varphi} + a_2 e^{-\sqrt{-\lambda}\varphi}$$

where a_1 and a_2 are constants.

$Q(\varphi)$ should be periodic, so λ must be positive and hence $Q(\varphi)$ assumes the following form

$$Q(\varphi) = a\cos(\sqrt{\lambda}\varphi) + b\sin(\sqrt{\lambda}\varphi) \tag{17}$$

where a and b are constants to be determined.

Given that $Q(\varphi)$ is an odd function, we have $a = 0$ and

$$Q = b\sin(\sqrt{\lambda}\varphi) \tag{18}$$

To guarantee $Q'(\varphi) \geq 0$ for $\varphi \in (-2\pi, 2\pi)$, b and λ should satisfy $b > 0$ and $0 \leq \lambda \leq \frac{1}{4}$.

Next we prove that $\lambda = \frac{1}{4}$ maximizes $\int_{-\pi}^{\pi} Q'^2(\varphi)d\varphi$ in (14). To this end, we only need to prove that $\int_{-\pi}^{\pi} Q'^2(\varphi)d\varphi$ is an increasing function of λ.

Substituting (18) into $\int_{-\pi}^{\pi} Q'^2(\varphi)d\varphi$ produces

$$\begin{aligned} f(\lambda) &\triangleq \int_{-\pi}^{\pi} \left(\frac{d(b\sin(\sqrt{\lambda}\varphi))}{d\varphi}\right)^2 d\varphi \\ &= \int_{-\pi}^{\pi} \left(b\sqrt{\lambda}\cos(\sqrt{\lambda}\varphi)\right)^2 d\varphi \\ &= b^2\left(\lambda\pi + \frac{\sqrt{\lambda}}{2}\sin(2\sqrt{\lambda}\pi)\right) \end{aligned} \tag{19}$$

Differentiating both sides of (19) by λ, we obtain

$$\frac{df(\lambda)}{d\lambda} = b^2\pi + b^2\frac{1}{4\sqrt{\lambda}}\sin(2\sqrt{\lambda}\pi) + \frac{b^2\pi}{2}\cos(2\sqrt{\lambda}\pi) \tag{20}$$

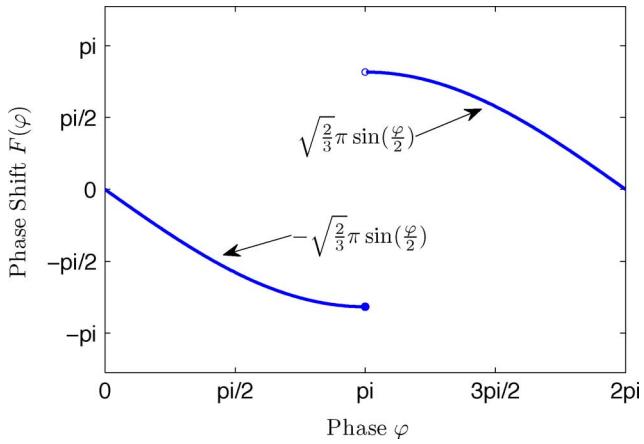

Fig. 2. The optimal phase response function for oscillators with non-identical natural frequencies.

which is always positive for $0 \leq \lambda \leq \frac{1}{4}$. Therefore, $f(\lambda)$ is an increasing function of λ and $\lambda = \frac{1}{4}$ gives the maximal $f(\lambda)$. Hence the optimal solution has the following form

$$Q(\varphi) = b\sin\left(\frac{\varphi}{2}\right) \tag{21}$$

We use the normalization constraint to determine b. Substituting (21) into the following normalization constraint

$$\int_{-\pi}^{\pi} Q^2(\varphi)d\varphi = C$$

produces $\int_{-\pi}^{\pi} b^2\sin^2(\frac{\varphi}{2}) = \pi b^2 = C$. So we have

$$b = \sqrt{\frac{C}{\pi}}$$

and

$$Q(\varphi) = \sqrt{\frac{C}{\pi}}\sin\left(\frac{\varphi}{2}\right) \tag{22}$$

Remark 5: The constant C in (22) can be regarded as a scaling factor and should be determined *a priori* for practical considerations. It does not affect the shape of the optimal phase response function that maximizes the synchronization rate.

Here, we determine C by using the constraint that the phase after pulsing perturbation still resides in $[0, 2\pi)$, i.e., $0 \leq F(\varphi) + \varphi < 2\pi$. Thus we have $0 \leq \varphi - Q(\varphi) < 2\pi$, which further means that $Q(\varphi) \leq \varphi$ holds for $0 \leq \varphi \leq \pi$ and $Q(\varphi) \geq -\varphi$ holds for $-\pi < \varphi \leq 0$. Therefore, we have $C = \int_{-\pi}^{\pi} Q^2(\varphi)d\varphi \leq \int_{-\pi}^{\pi} \varphi^2 d\varphi = \frac{2\pi^3}{3}$. Setting C as $\frac{2\pi^3}{3}$, we have the optimal $Q(\varphi)$ as

$$Q(\varphi) = \sqrt{\frac{2}{3}}\pi\sin\left(\frac{\varphi}{2}\right) \tag{23}$$

Summarizing the above derivation, we get the optimal phase response function $F(\varphi)$:

Theorem 4: For PCOs with constant non-identical natural frequencies, the optimal phase response function that maximizes the rate of frequency synchronization is given by

$$F(\varphi) = \begin{cases} -\sqrt{\frac{2}{3}}\pi\sin\left(\frac{\varphi}{2}\right) & 0 \leq \varphi \leq \pi \\ \sqrt{\frac{2}{3}}\pi\sin\left(\frac{\varphi}{2}\right) & \pi < \varphi < 2\pi \end{cases} \tag{24}$$

Proof: Using the periodicity of $Q(\varphi)$ and its relation with $F(\varphi)$, the theorem can be easily obtained. ■

The optimal phase response function is visualized in Fig. 2.

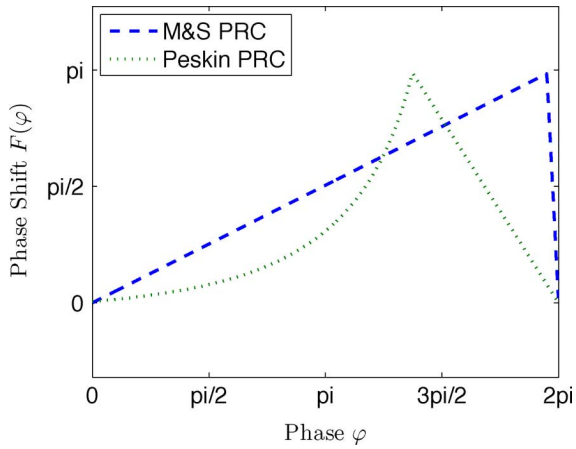

Fig. 3. The shapes of the Peskin phase response function (Peskin PRC) and the M&S phase response function (M&S PRC).

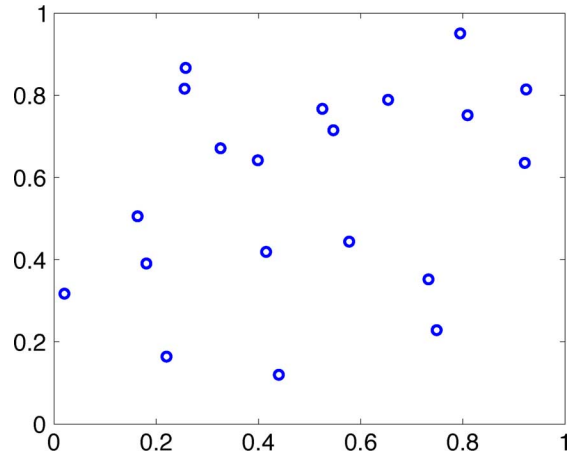

Fig. 4. The distribution of nodes in the random geometric graph used in simulation.

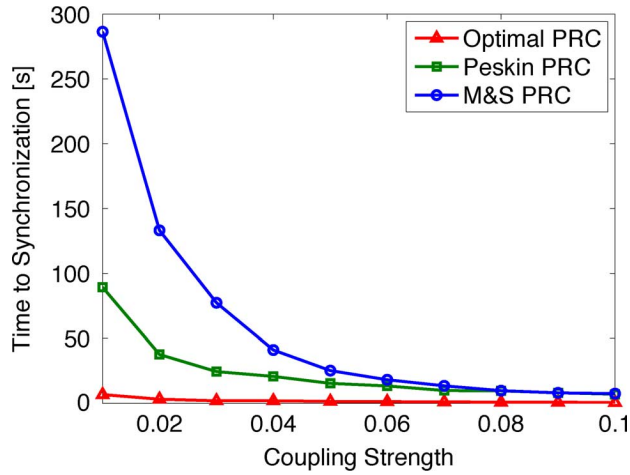

Fig. 5. Time to synchronization for different phase response functions in the identical natural frequency case.

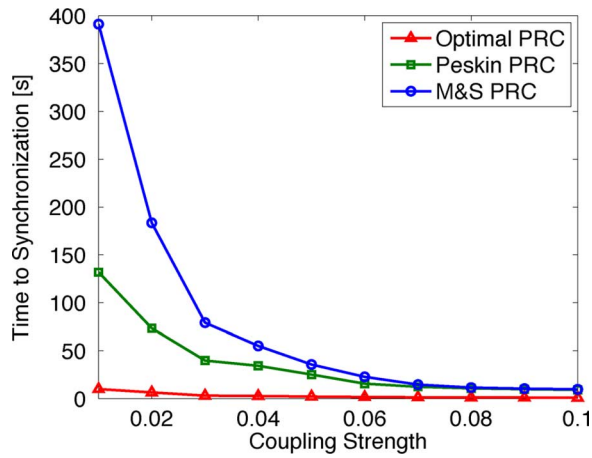

Fig. 6. Time to frequency synchronization for different phase response functions in the non-identical natural frequency case.

V. Comparison With Existing Phase Response Functions

We confirm the optimality of our phase response functions by comparing them with the commonly used phase response functions (the Peskin phase response function used in [5] and the M&S phase response function used in [7], [8]) in terms of time to synchronization. The shapes of the Peskin phase response function and the M&S phase response function are given in Fig. 3.

We considered a network composed of 20 PCOs. The oscillators are deployed in a plane with 2-dimensional coordinates randomly chosen from a uniform distribution. Any two nodes within 0.35 unit distance can interact with each other. The random geometric graph used in simulation is given in Fig. 4 and it is verified that the interaction topology is connected.

To show the optimality of our phase response function, we compared its time to synchronization with the time to synchronization under phase response functions 'Peskin PRC' given in [5] and 'M&S PRC' given in [7], [8]. We define synchronization to be achieved when all nodes fire at the same time. For each phase response function, we simulated the network under different coupling strengths l. For each given coupling strength, we ran the simulation for 100 times and each time we chose the initial phases randomly from the uniform distribution on $[0, \pi)$. The time to synchronization is defined to be the average over the 100 runs. When all oscillators have identical natural frequencies $w_1 = w_2 = \cdots = w_{21} = 1$ Hz, the times to synchronization under different coupling strengths for the three phase response functions are given in Fig. 5. It is clear that our optimal phase response function gives the fastest rate of synchronization.

We also simulated the network in the non-identical natural frequency case. The simulation setup is the same as the identical-natural frequency case except that the initial phases were randomly chosen from $[0, 2\pi)$ and deviations randomly chosen from the interval $[-0.01, 0.01]$ were added to the natural frequencies. The times to frequency synchronization for the three phase response functions under different coupling strengths are given in Fig. 6. It is clear that the optimal phase response function derived in Section IV gives a faster rate of frequency synchronization compared with the currently most commonly used phase response functions.

VI. Conclusion

Pulse-coupled synchronization strategies have attracted increased attention in wireless sensor networks. We propose to maximize the synchronization rate by optimizing the phase response function. This can increase the synchronization rate with coupling strengths fixed, and hence can reduce the time to synchronization with the transmission power fixed. Given that the energy consumption is determined by the product of the transmission power and the time to synchronization, the optimal phase response function can reduce energy consumption in synchronization. This has great significance for wireless sensor networks where energy is a valuable system resource.

REFERENCES

[1] C. S. Peskin, "Mathematical aspects of heart physiology," Courant Inst. of Math. Sci., New York, 1975.

[2] R. Mirollo and S. Strogatz, "Synchronization of pulse-coupled biological oscillators," *SIAM J. Appl. Math.*, vol. 50, pp. 1645–1662, 1990.

[3] C. Canavier and S. Achuthan, "Pulse coupled oscillators and the phase resetting curve," *Math. Biosci.*, vol. 226, pp. 77–96, 2010.

[4] R. Mathar and J. Mattfeldt, "Pulse-coupled decentral synchronization," *SIAM J. Appl. Math.*, vol. 56, pp. 1094–1106, 1996.

[5] Y. W. Hong and A. Scaglione, "A scalable synchronization protocol for large scale sensor networks and its applications," *IEEE J. Sel. Areas Commun.*, vol. 23, no. 5, pp. 1085–1099, 2005.

[6] Y. Q. Wang, F. Núñez, and F. J. Doyle, III, "Energy-efficient pulse-coupled synchronization strategy design for wireless sensor networks through reduced idle listening," *IEEE Trans. Signal Process.*, vol. 60, no. 10, pp. 5293–5306, Oct. 2012.

[7] G. Werner-Allen, G. Tewari, A. Patel, M. Welsh, and R. Nagpal, "Firefly inspired sensor network synchronicity with realistic radio effects," in *Proc. SenSys*, 2005, pp. 142–153.

[8] A. Hu and S. D. Servetto, "On the scalability of cooperative time synchronization in pulse-connected networks," *IEEE Trans. Inf. Theory*, vol. 52, no. 6, pp. 2725–2748, 2006.

[9] R. Pagliari and A. Scaglione, "Scalable network synchronization with pulse-coupled oscillators," *IEEE. Trans. Mobile Comput.*, vol. 10, no. 3, pp. 392–405, 2011.

[10] K. Konishi and H. Kokame, "Synchronization of pulse-coupled oscillators with a refractory period and frequency distribution for a wireless sensor network," *Chaos*, vol. 18, p. 033132, 2008.

[11] T. Okuda, K. Konishi, and N. Hara, "Experimental verfication of synchronization in pulse-coupled oscillators with a refractory period and frequency distribution," *Chaos*, vol. 21, p. 023105, 2011.

[12] E. M. Izhikevich, *Dynamical Systems in Neuroscience: The Geometry of Excitability and Bursting*. London, U.K.: MIT Press, 2007.

[13] C. H. Johnson, "Forty years of PRCs—What have we learned?," *Chronobiol. Int.*, vol. 16, pp. 711–743, 1999.

[14] S. Marella and G. B. Ermentrout, "Class-II neurons display a higher degree of stochastic synchronization than Class-I neurons," *Phys. Rev. E*, vol. 77, p. 041918, 2008.

[15] F. C. Hoppensteadt and E. M. Izhikevich, *Weakly Connected Neural Networks*. New York: Springer, 1997.

[16] Y. Q. Wang, F. Núñez, and F. J. Doyle, III, "Increasing sync rate of pulse-coupled oscillators via phase response function design: Theory and application to wireless networks," *IEEE Trans. Control Syst. Technol.*, 2012, doi: 10.1109/TCST.2012.2205254, available as preprint.

[17] T. S. Rappaport, *Wireless Communications: Principles and Practice*. Englewood Cliffs, NJ: Prentice-Hall, 2002.

[18] J. Guckenheimer and P. Holmes, *Nonlinear Oscillations, Dynamical Systems and Birfurcations of Vector Fields*. New York: Springer-Verlag, 1986.

[19] C. V. Vreeswijk, L. F. Abbott, and G. B. Ermentrout, "When inhibition not excitation synchronizes neural firing," *J. Comput. Neurosci.*, vol. 1, pp. 313–321, 1994.

[20] Y. Q. Wang and F. J. Doyle, III, "On influences of global and local cues on the rate of synchronization of oscillator networks," *Automatica*, vol. 47, pp. 1236–1242, 2011.

[21] A. E. Brouwer and W. H. Haemers, *Spectra of Graphs*. New York: Springer, 2012.

[22] E. Mallada and A. Tang, "Synchronization of phase-coupled oscillators with arbitrary topology," in *Proc. Amer. Control Conf.*, Baltimore, MD, 2010, pp. 1777–1782.

[23] A. S. Tanenbaum, *Computer Networks*. Englewood Cliffs, NJ: Prentice-Hall, 2003.

[24] S. Strogatz, "From Kuramoto to Crawford: Exploring the onset of synchronization in populations of coupled oscillators," *Phys. D, Nonlin. Phenom.*, vol. 143, pp. 1–20, 2000.

[25] N. Varanese, U. Spagnolini, and Y. Bar-Ness, "Distributed frequency-locked loops for wireless networks," *IEEE Trans. Commun.*, vol. 59, no. 12, pp. 3440–3451, 2011.

[26] P. Parker, P. Mitran, D. Bliss, and V. Tarokh, "On bounds and algorithms for frequency synchronization for collaborative communication systems," *IEEE Trans. Signal Process.*, vol. 56, no. 8, pp. 3742–3752, 2008.

An Extension of a Calibration-Free Trajectory Reconstruction Method for Wireless Networks

Anthony Almudevar and Jason Lacombe

***Abstract*—A signal processing algorithm for the estimation of the trajectory of a mobile transmitter in a wireless network, based on RSSI measurements, was proposed in [A. Almudevar, "Approximate calibration-free trajectory reconstruction in a wireless network," *IEEE Trans. Signal Process.*, vol. 56, no. 7, pp. 3081–3088, 2008]. The problem of explicit transmission source location estimation is bypassed, producing instead an estimation of the trajectory shape which does not require a translation of RSSI measurements into transmission distance estimates. It was proven for the case of $k = 3$ receivers that the resulting mapping of the source to an estimation region is $1-1$ and continuous while preserving directionality and providing robustness to measurement distortion. The purpose of this correspondence is to extend these results to the general $k \geq 3$ case. The method is demonstrated using a commercial RSSI home monitoring system using $k = 4$ receivers.**

***Index Terms*—Location estimation, tracking, wireless networks.**

I. INTRODUCTION

Location and motion monitoring within sensor networks is an active area of research. Much work has focused on indoor environments where objects and barriers interfere with signal transmission. A calibration-free approach to this problem was proposed in Almudevar [1], in which the shape of a trajectory, rather than an explicit location, is estimated. By foregoing the problem of direct location estimation, difficulties associated with calibration or installation procedures are avoided.

We assume that a wireless network of k stationary receivers is installed in region $T_0 \subset \mathcal{R}^2$. Time stamped RSSI measurements induced by a mobile transmitter at $\mathbf{x} \in T_0$ are captured at each receiver. An RSSI measurement at the ith receiver is transformed into a *distance analog* $d_i \in \mathcal{D}$, where $\mathcal{D}$ is the measurement range, resulting in a distance vector $\mathbf{d} = (d_1, \ldots, d_k) \in \mathcal{D}^k$ of synchronized measurements. It is important to note that d_i need not be a transmission distance estimate, but it should decrease as the ith receiver is approached. The simplest approach will be to let d_i be a decreasing function of the RSSI measurement. This gives an implicit mapping $H_0 : T_0 \rightarrow \mathcal{D}^k$ based on the sequence $\mathbf{x} \rightarrow \text{RSSI} \rightarrow \mathbf{d}$. Then the signal processing algorithm H_1, developed here, maps $\mathbf{d}$ into an estimation plane $T_1 \subset \mathcal{R}^2$, generating the estimated trajectory. This yields the implicit compound

Manuscript received November 30, 2011; revised March 28, 2012 and May 16, 2012; accepted May 19, 2012. Date of publication June 08, 2012; date of current version September 11, 2012. The associate editor coordinating the review of this manuscript and approving it for publication was Prof. Huaiyu Dai. The project described in this publication was supported by a Novel Biostatistical Methodology Pilot Award from the University of Rochester CTSA award number UL1 RR024160 from the National Center for Research Resources and the National Center for Advancing Translational Sciences of the National Institutes of Health. The content is solely the responsibility of the authors and does not necessarily represent the official views of the National Institutes of Health. Additional funding was provided by the Everyday Technologies for Alzheimer Care (ETAC) initiative of the Alzheimer's Association, and by the Center for Future Health, University of Rochester. The monitoring equipment was provided by Home Free Systems Limited.

A. Almudevar is with the Department Biostatistics and Computational Biology, University of Rochester, Rochester, NY 14642 USA (e-mail: anthony_almudevar@urmc.rochester.edu).

J. Lacombe is with Nature Source Genetics, Ithaca NY 14850-1275 USA (e-mail: jlacombe@naturesourcegenetics.com).

Digital Object Identifier 10.1109/TSP.2012.2203817